

Vortices in Josephson arrays interacting with non-classical microwaves: The effect of dissipation

A. Konstadopoulou^{1,a}, J.M. Hollingworth³, M. Everitt², A. Vourdas¹, T.D. Clark², and J.F. Ralph³

¹ Department of Computing, University of Bradford, Bradford BD7 1DP, UK

² School of Engineering and Information Technology, University of Sussex, Falmer, Brighton BN1 9QT, UK

³ Department of Electrical Engineering and Electronics, University of Liverpool, Liverpool L69 3GJ, UK

Received 21 October 2002 / Received in final form 11 February 2003

Published online 11 April 2003 – © EDP Sciences, Società Italiana di Fisica, Springer-Verlag 2003

Abstract. Vortices circulating in a ring made from a Josephson array in the insulating phase are studied. The ring contains a ‘dual Josephson junction’ through which the vortices tunnel. External non-classical microwaves are coupled to the device. The time evolution of this two-mode fully quantum mechanical system is studied, taking into account the dissipation in the system. The effect of the quantum statistics of the photons on the quantum statistics of the vortices is discussed. Entropic calculations quantify the entanglement between the two systems. Quantum phenomena in the system are also studied through Wigner functions. After a certain time (which depends on the dissipation parameters) these quantum phenomena are destroyed due to dissipation.

PACS. 74.50.+r Tunneling phenomena; point contacts, weak links, Josephson effects – 85.25.Dq Superconducting quantum interference devices (SQUIDs) – 42.50.Dv Nonclassical states of the electromagnetic field, including entangled photon states; quantum state engineering and measurements

1 Introduction

There has been a lot of interest in coherent electron behaviour in Josephson devices for a long time. The new development in the last ten years [1] has been the experimental and theoretical study of mesoscopic Josephson devices (small Josephson junctions with low capacitance) where quantum phenomena are stronger.

Coherent vortex behaviour in insulating systems (realised with Josephson arrays made from superconducting islands coupled through Josephson junctions) has also been studied in the literature [2–5]. There is a duality between electrons in the superconducting phase and vortices in the insulating phase which has been studied in [6, 7]. Similar duality has been studied in various branches of physics (Krammers-Wannier duality [8], t’Hooft duality in Gauge theories [9], duality in quantum hair of black holes [10], etc.). The superinsulator state, which is a coherent superposition of suitable vortex number states, is the quantum dual of the well known superconducting state, which is a coherent superposition of suitable electron pair number states. Superinsulators are based on vortex condensates in dual way to the Cooper pair condensates in Josephson junctions. In superinsulators vortices move with high mobility in an analogous way to the

Cooper pairs in superconductors. We stress that the terminology indicates the behaviour of electric charges; while the behaviour of vortices is the opposite. For example the superconductors conduct electric charges and insulate vortices. The insulators insulate electric charges (because the Coulomb coupling constant E_C is greater than the Josephson coupling constant E_J and it requires a lot of energy for electrons to move from one superconducting island to the next one); and conduct vortices (superconduct in the case of negligible dissipation).

Two condensates close to each other can lead to Josephson junction phenomena. Two weakly linked vortex condensates lead to ‘dual Josephson junctions’ for vortices which have been studied in reference [11]. They are weak links between two ‘superinsulators’ and vortices tunnel through them in an analogous (dual) way to the tunneling of electron pairs through weak links between two superconductors (Josephson junctions).

At the same time there has been significant developments in quantum optics. Non-classical electromagnetic fields have been studied extensively both experimentally and theoretically. These fields are carefully prepared in a particular quantum state so that the amount of quantum noise is well defined and the statistics of photons is also well defined.

In this paper we consider a ring made from a Josephson array in insulating phase. The vortex mass is inversely

^a e-mail: a.konstadopoulou@brad.ac.uk

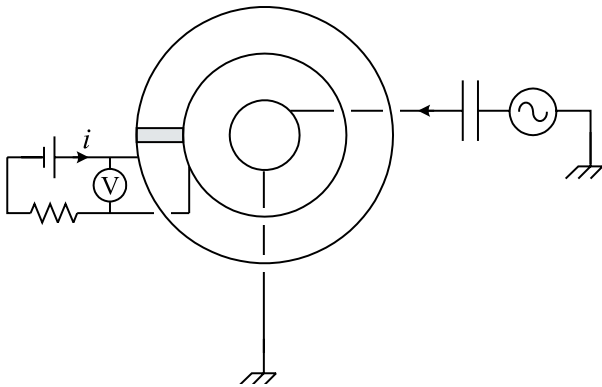


Fig. 1. A Josephson array ring in the insulating phase, coupled to a source of non-classical microwaves. The ring contains a dual Josephson junction (*i.e.* a Josephson junction for vortices). The voltmeter measures the vortex current. The current i compensates the dissipation. The centre of the ring contains charge $Q(t)$ induced through coupling with a cylindrical waveguide in the TM_{01} mode.

proportional to E_C and is very low so that the vortices behave as quantum particles. In this case vortices circulate this ring with high mobility. The ring contains a dual Josephson Junction through which the vortices tunnel. The system interacts with non-classical microwaves (at GHz-THz frequencies) [12]. This is a fully quantum mechanical system and we study explicitly how the quantum noise of the electromagnetic fields affects the quantum noise of the vortex current. Preliminary results on this system in the absence of dissipation, have been presented in reference [13]. In this paper we extend further this work taking into account the dissipation in the system. The results show that interesting quantum phenomena occur up to a certain time. They include nonclassical statistics (for both the device and the microwaves), entanglement between the two modes, etc. After a certain time dissipation destroys these phenomena.

Josephson systems are good candidates for the development of amplifiers and frequency converters operating at THz frequencies, which is the modern tendency in Communications. There is also a lot of work currently, for their use as quantum gates in Quantum Technology and Quantum Computing [14]. Nonclassical states in Josephson systems have been produced experimentally in [15].

2 Interaction of Josephson arrays with external non-classical microwaves

We consider a ring (Fig. 1) made from an array of Josephson junctions with Coulomb coupling constant E_C greater than the Josephson coupling constant E_J . For those values of the parameters the array is in the insulating phase where vortices move with high mobility and charges are confined. Such rings have been considered experimentally in the context of the Aharonov-Casher effect in reference [5].

However, our ring has also a ‘dual Josephson junction’ [11]. This plays a similar role for vortices, to the ordinary Josephson junctions for electron pairs. The ‘dual phase’ of the vortex wavefunction has a phase difference δ along the dual Josephson junction. This is analogous to the Cooper-pair wavefunction in superconducting rings with Josephson junctions which has phase difference ϕ along the junction. The centre of the ring contains charge $Q(t)$ induced through coupling with an external source of microwaves which are carefully prepared in a particular quantum state. For example we can put the device of Figure 1 in a cylindrical waveguide in the TM_{01} mode with the plane of the diagram perpendicular to the axis of the cylinder.

Microwaves in various quantum states have been produced experimentally in several laboratories. The system operates at low temperatures ($\hbar\Omega_1 > k_B T$ and $\hbar\Omega_2 > k_B T$), so that the thermal noise is less than the quantum noise in the microwaves and the device.

The Hamiltonian that describes this device has an inductive, a capacitive and a ‘dual Josephson’ part. The inductive part is

$$H_{ind} = \frac{1}{2}LI^2 + \frac{1}{2}L_{mw}I_{mw}^2 - gII_{mw} \quad (1)$$

where L is inductance of the device, L_{mw} is the inductance of the circuit that produces the external microwaves and g is the mutual inductance between the two circuits. For simplicity we assume that $L = L_{mw}$ and that we have maximum coupling between the two circuits so that $g = \sqrt{LL_{mw}} = L$. I and I_{mw} are the total and external (microwave) current correspondingly, flowing in the radial direction of the device. In this case the above inductive term of Hamiltonian can be written as

$$H_{ind} = \frac{1}{2}L(I - I_{mw})^2 = \frac{1}{2L}(\Phi - \Phi_{mw})^2. \quad (2)$$

Making similar assumptions for the capacitive part of the Hamiltonian we write it as

$$H_{cap} = \frac{(Q - Q_{mw})^2}{2C} \quad (3)$$

where C is the capacitance between the inner and outer boundaries of the ring. Q and Q_{mw} are the total and external (microwave) charge correspondingly, in the inner boundary of the ring. The ‘dual’ Josephson part of the Hamiltonian is in general

$$H_{dJ} = E_{dJ}(1 - \cos \delta) \quad (4)$$

E_{dJ} is the dual Josephson coupling constant and $\delta = \Phi_0 Q$ the dual phase. $\Phi_0 = \pi/e$ is the flux quantum (in units where $\hbar = k_B = c = 1$). The sinusoidal term $E_{dJ}(1 - \cos \delta)$ describes vortex tunnelling through the dual Josephson junction. This is analogous to the well-known term $E_J(1 - \cos \phi)$ which describes the tunnelling of electron pairs in Josephson junctions. The total Hamiltonian of the system is

$$H = \frac{1}{2}L(I - I_{ex})^2 + \frac{(Q - Q_{ex})^2}{2C} + E_{dJ}(1 - \cos \delta). \quad (5)$$

The system comprises of two coupled oscillators. The first is the Josephson device which behaves as a non-linear $L-C$ circuit with frequency $\Omega_1 = (LC)^{-1/2}$. Quantization of the device is done with the creation and annihilation operators

$$a_1 = \left(\frac{1}{2\Omega_1 C} \right)^{1/2} [Q + i\Omega_1^{-1}I], \quad (6)$$

$$a_1^\dagger = \left(\frac{1}{2\Omega_1 C} \right)^{1/2} [Q - i\Omega_1^{-1}I], \quad (7)$$

$$[a_1, a_1^\dagger] = 1. \quad (8)$$

We note that $\Omega_1 = (LC)^{-1/2}$ is the frequency of the linear part of the device. The sinusoidal non-linearity renormalises this frequency (*i.e.*, there is an $a_1^\dagger a_1$ term within the $\cos \delta$ non-linearity). The electromagnetic field is quantized with the operators:

$$a_2 = \left(\frac{1}{2\Omega_2 C} \right)^{1/2} [Q_{mw} + i\Omega_2^{-1}I_{mw}], \quad (9)$$

$$a_2^\dagger = \left(\frac{1}{2\Omega_2 C} \right)^{1/2} [Q_{mw} - i\Omega_2^{-1}I_{mw}], \quad (10)$$

$$[a_2, a_2^\dagger] = 1 \quad (11)$$

where $\Omega_2 = (LC)^{-1/2}$ is the frequency of the microwaves. We note that for the parameters considered $\Omega_1 = \Omega_2$.

The Hamiltonian can now be written as

$$H = \Omega_1 a_1^\dagger a_1 + \Omega_2 a_2^\dagger a_2 - E_{dJ} \cos \left[\mu (a_1^\dagger + a_1) \right] - \Omega_1 (a_1^\dagger a_2 + a_1 a_2^\dagger) \quad (12)$$

where $\mu = \Phi_0(\Omega_1 C/2)^{1/2}$.

3 Time evolution

In the presence of dissipation (*e.g.* [16]) the density matrix of the system $\rho(t)$ is given by

$$\begin{aligned} \frac{\partial \rho}{\partial t} = & i[H, \rho] + \frac{\gamma_1}{2}(M+1) (2a_1 \rho a_1^\dagger - a_1^\dagger a_1 \rho - \rho a_1^\dagger a_1) \\ & + \frac{\gamma_1}{2}M (2a_1^\dagger \rho a_1 - a_1 a_1^\dagger \rho - \rho a_1 a_1^\dagger) \\ & + \frac{\gamma_2}{2}(M+1) (2a_2 \rho a_2^\dagger - a_2^\dagger a_2 \rho - \rho a_2^\dagger a_2) \\ & + \frac{\gamma_2}{2}M (2a_2^\dagger \rho a_2 - a_2 a_2^\dagger \rho - \rho a_2 a_2^\dagger), \end{aligned} \quad (13)$$

where $\rho(0)$ is the density matrix at $t=0$. γ is the damping rate and M is the average number of bath quanta. For a monochromatic bath with frequency ω_B in thermal equilibrium at temperature T ,

$$M(\omega_B) = \left(e^{\omega_B/T} - 1 \right)^{-1}. \quad (14)$$

This is a simple model for dissipation. It takes into account the effect of the environment on system which will be placed in a cavity (with a large but finite Q -value). There are of course many sources of dissipation in such a complex system. The above model is an effective formalism which can be used to describe collectively the effect of various sources of dissipation. Experimentalists can use the numerical results of this model to fit their data and extract the values of the parameters γ_1 , γ_2 , M describing in this way the very complex phenomenon of dissipation in this system, with three parameters.

Details for the numerical solution of equation (13) are given in the appendix. We have calculated numerically $\rho(t)$ and the reduced density matrices

$$\rho_1(t) = \text{Tr}_2 \rho(t); \quad \rho_2(t) = \text{Tr}_1 \rho(t). \quad (15)$$

Using the reduced density matrices we calculated the average number of quanta in each mode

$$\langle N_i \rangle = \text{Tr} [a_i^\dagger a_i \rho_i] \quad (16)$$

as functions of time.

The infinite dimensional matrix $\langle M_1, M_2 | H | N_1, N_2 \rangle$ has been truncated for the numerical calculations, with M_1, N_1 taking values from 0 up to K_{1max} and M_2, N_2 taking values from 0 up to K_{2max} . Correspondingly, K_{1max} and K_{2max} were taken to be much greater than $\langle N_1 \rangle$ and $\langle N_2 \rangle$. As a measure of the accuracy of the approximation we calculated the traces of the truncated matrices. In the limit $K_{1max} \rightarrow \infty$ and $K_{2max} \rightarrow \infty$ they equal to 1; and in the truncated case they should be very close to 1. In all our results the above sum was greater than 0.98.

4 Quantum statistics and quantum noise

The microwaves have been carefully prepared in a quantum state and this implies that the quantum statistics of the photons threading the ring, is known. In our analysis we study a ‘Quantum Faraday Law’ and investigate how the quantum statistics and quantum noise of the photons affects the quantum statistics and quantum noise of the tunneling vortices. In order to quantify the quantum statistics, we calculate the second order correlations

$$g_{ii}^{(2)} = \frac{\langle N_i^2 \rangle - \langle N_i \rangle^2}{\langle N_i \rangle^2}; \quad i = 1, 2, \quad (17)$$

$$g_{12}^{(2)} = \frac{\langle N_1 N_2 \rangle}{\langle N_1 \rangle \langle N_2 \rangle}, \quad (18)$$

and the ratio

$$r = \frac{[g_{12}^{(2)}]^2}{g_{11}^{(2)} g_{22}^{(2)}}. \quad (19)$$

The $g_{11}^{(2)}$ describe vortex bunching or antibunching; and the $g_{22}^{(2)}$ describe photon bunching or antibunching. The quantum noise is quantified with the uncertainties

$$(\Delta x_i)^2 = \text{Tr} (\rho x_i^2) - [\text{Tr} (\rho x_i)]^2; \quad i = 1, 2 \quad (20)$$

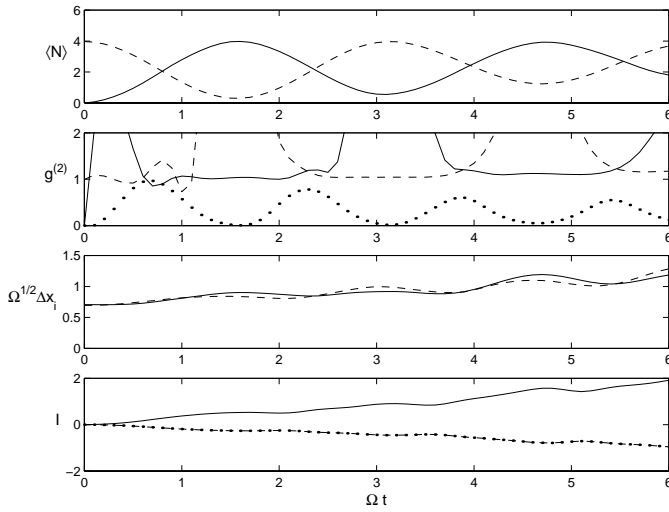


Fig. 2. At time $t = 0$ the device is in the lowest (vacuum) state $|N = 0\rangle$ and the microwaves in the coherent state $|A = 2\rangle$. Results are in the absence of dissipation.

5 Entanglement

At $t = 0$ the system is not entangled, but as time evolves the microwaves entangle with the Josephson array device. As a measure of the correlations between the two modes we have calculated the entropy [17]

$$I = S(\rho_1) + S(\rho_2) - S(\rho), \quad (21)$$

where $S = -\text{Tr} \rho \ln \rho$ is the von Neumann entropy. The entanglement entropy I is positive according to the subadditivity property. The results show that although originally the two modes are uncorrelated, they become strongly correlated later. These correlations might be classical or quantum mechanical (entanglement). Reference [18] have used the conditional entropies

$$\begin{aligned} I_1 &= -S(\rho_1) + S(\rho) \\ I_2 &= -S(\rho_2) + S(\rho) \end{aligned} \quad (22)$$

as a criterion for entanglement. When $I_i < 0$ ($i = 1, 2$) the system is entangled (although the converse is not true, *i.e.*, an entangled system might have $I_i > 0$).

If the system is in a pure state at $t = 0$ and evolves unitarily in a dissipationless environment then $S(\rho) = 0$ and $S(\rho_1) = S(\rho_2)$. In this case $I = -2I_1 = -2I_2$ and therefore a positive value of I indicates a negative value of I_i and hence entanglement.

6 Results

In Figure 2 we assume that at time $t = 0$ the device is in the lowest (vacuum) state $|0\rangle$ ($a_1|0\rangle = 0$) and the microwaves in the coherent state $|A = 2\rangle$ ($a_2|A\rangle = A|A\rangle$). $\Omega_1 = \Omega_2 = 1.5 \times 10^{-4}$, $E_{dJ} = 10^{-4}$, $\mu = 2.8408$ and truncation $K_{i,max} = 10$. In these results there is no dissipation ($\gamma_1 = \gamma_2 = 0$). The first graph shows $\langle N_1 \rangle$ (solid

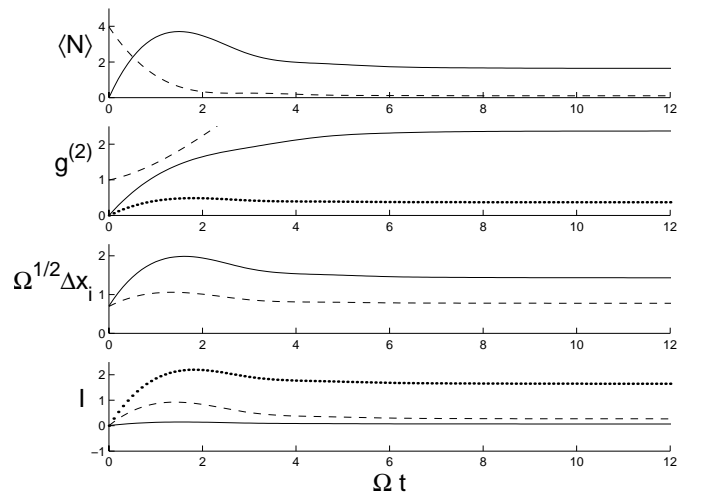


Fig. 3. Results for the model of Figure 2 with dissipation $\gamma_1 = 2 \times 10^{-4}$, $\gamma_2 = 10^{-4}$ and $M = 1$.

line) and $\langle N_2 \rangle$ (broken line) as functions of time. The results show the exchange of energy between the two modes. The second graph shows $g_{11}^{(2)}$ (solid line), $g_{22}^{(2)}$ (broken line) and r (dotted line) as functions of time. It is seen that when one of the modes is described by Poissonian statistics ($g^{(2)} = 1$) the other mode is described by super-Poissonian statistics (strong bunching). These two statistics are exchanged almost periodically as functions of time. The third graph shows the uncertainties $\sqrt{\Omega} \Delta x_1$ (solid line) and $\sqrt{\Omega} \Delta x_2$ (dotted line) as functions of time. The fourth graph shows the entropies I (solid line), I_1 (broken line) and I_2 (dotted line) in natural units (nats) as a function of time. As we explained above since in this example at $t = 0$ the system is in a pure state and there is no dissipation, $I = -2I_1 = -2I_2$. The results show that we have strong entanglement.

In Figure 3 we show results for the model of Figure 2 with dissipation $\gamma_1 = 2 \times 10^{-4}$, $\gamma_2 = 10^{-4}$ and $M = 1$. The results show clearly the destructive role of dissipation on quantum phenomena. After some time, there is no exchange of energy between the two modes, the statistics is thermal or even ‘super-thermal’ and there is no entanglement. Comparison of the entanglement results in Figure 2 (no dissipation) and in Figure 3 (with dissipation) shows that the dissipation after some time destroys the entanglement. Indeed, in the absence of dissipation (Fig. 2) the quantity $I = -2I_1 = -2I_2$ is an increasing function of time. In contrast in the presence of dissipation (Fig. 3) the same quantity very quickly becomes almost zero.

In order to see clearly the effect of dissipation we have calculated the Wigner function defined as the Wigner function of an ‘arbitrary’ operator Θ (in our case the density matrices)

$$\Theta = \sum_{N,M} \Theta_{NM} |N\rangle \langle M| \quad (23)$$

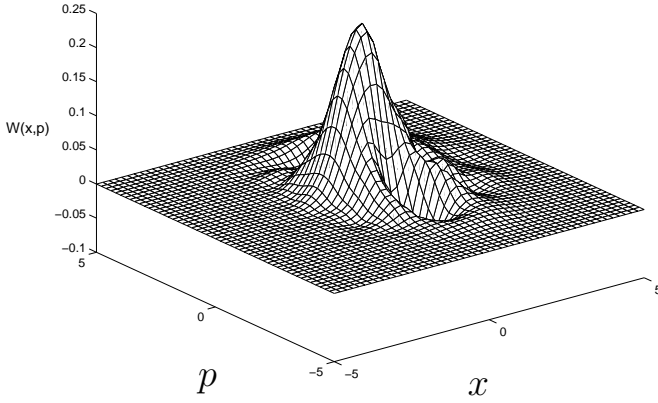


Fig. 4. The Wigner function for the state of the device at $\Omega_1 t = 6$ for the model of Figure 2 with no dissipation.

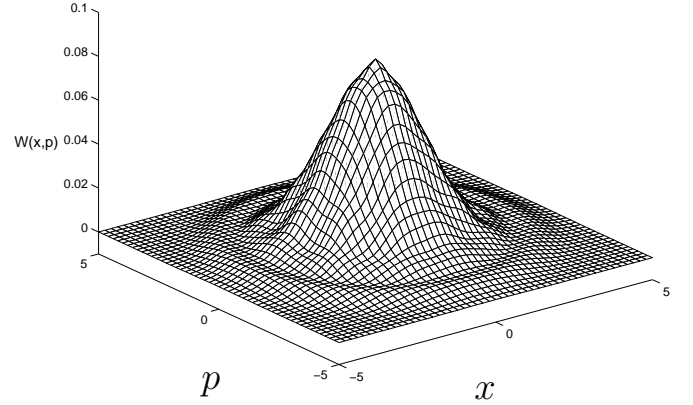


Fig. 6. The Wigner function for the state of the device at $\Omega_1 t = 6$ for the model of Figure 2 with dissipation $\gamma_1 = 2 \times 10^{-4}$, $\gamma_2 = 10^{-4}$ and $M = 1$.

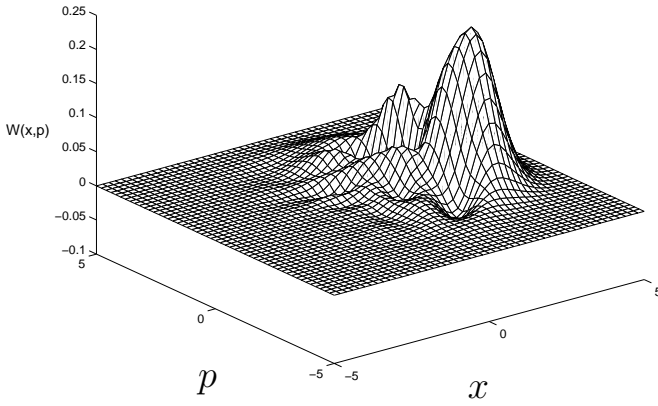


Fig. 5. The Wigner function for the state of the microwaves at $\Omega_2 t = 6$ for the model of Figure 2 with no dissipation.

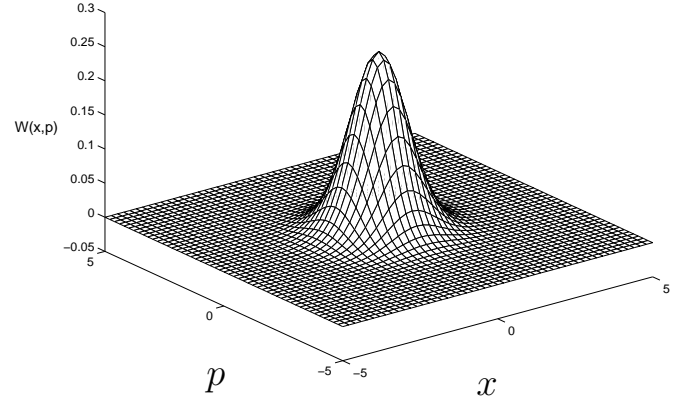


Fig. 7. The Wigner function for the state of the microwaves at $\Omega_2 t = 6$ for the model of Figure 2 with dissipation $\gamma_1 = 2 \times 10^{-4}$, $\gamma_2 = 10^{-4}$ and $M = 1$.

is defined as

$$\begin{aligned} W(x,p) &= \frac{1}{2\pi} \int dX \left\langle x + \frac{1}{2}X | \Theta | x - \frac{1}{2}X \right\rangle \exp(-ipX) \\ &= \sum_{N,M} \Theta_{NM} W_{MN}(x,p) \end{aligned} \quad (24)$$

where

$$\begin{aligned} W_{MN}(x,p) &= \frac{(-1)^N}{\pi} \left(\frac{N!}{M!} \right)^{1/2} \left[2^{1/2}(x+ip) \right]^{M-N} \\ &\quad \times \exp(-x^2 - p^2) L_N^{M-N}(2x^2 + 2p^2) \end{aligned} \quad (25)$$

and L_N^{M-N} are Laguerre polynomials.

In Figure 4 the Wigner function for the state of the device at $\Omega_1 t = 6$ for the model of Figure 2 with no dissipation. In Figure 5 we show the Wigner function for the state of the microwaves at $\Omega_2 t = 6$ for the model of Figure 2 with no dissipation. In Figure 6 we show the Wigner function for the state of the device at $\Omega_1 t = 6$ for the model of Figure 2 with dissipation $\gamma_1 = 2 \times 10^{-4}$, $\gamma_2 = 10^{-4}$ and $M = 1$. In Figure 7 the Wigner function for the state of the microwaves at $\Omega_2 t = 6$ for the model of Figure 2 with dissipation $\gamma_1 = 2 \times 10^{-4}$, $\gamma_2 = 10^{-4}$ and $M = 1$. Figures 6 and 7 show that both modes are described by

almost Gaussian Wigner functions which are characteristic of thermal states. This is not the case for Figures 4 and 5 where there is no dissipation. So after some time dissipation thermalises both modes. This can also be seen from the values of $g^{(2)}$, but the Wigner functions show it very clearly in the position momentum plane.

We note that similar behaviour with our model is exhibited by other models like for example the Jaynes-Cummings model [19] which describes the interaction of light with Rydberg atoms. We stress however that Josephson models have strong sinusoidal non-linearity.

7 Discussion

We have considered a ring made from a Josephson array in the insulating phase. The ring contains a dual Josephson junction through which the vortices tunnel. From a mathematical point of view the dual Josephson junction is described with a sinusoidal non-linear term. External non-classical microwaves are coupled to the device. The work explores dual Josephson junctions and dual Josephson phenomena with vortex condensates.

We have calculated the time evolution of this fully quantum mechanical two-mode system in the presence of dissipation. The results have shown that for short times, there is an exchange of energy between the microwaves and the vortices. We have also studied quantitatively (with the $g^{(2)}$) how the quantum noise of the electromagnetic field affects the quantum noise of the vortices; and how the two modes become entangled. However, all these important quantum phenomena occur only for short time after which the dissipation dominates. The results answer quantitatively the practically important question of how long the coherence is preserved.

Our model can be useful in the context of quantum gates based on Josephson technology; and also in the context of THz technology.

A.K. gratefully acknowledges support from EPSRC.

Appendix

We solve the truncated equation (13) by converting it into the form

$$\frac{dr}{dt} = \mathcal{A}r, \quad (26)$$

where r is a ‘density vector’, and \mathcal{A} is an ‘appropriate’ matrix.

By ‘density vector’ we mean a vector representation of the truncated density matrix $\rho_{mn\kappa\lambda}$. Our density matrix is four dimensional and after truncation it has $(K_{max}+1)^4$ elements. Using the built-in function *reshape* in MATLAB, this matrix has been converted in a first stage into a two dimensional matrix and then into a one-dimensional vector r [20].

The matrix \mathcal{A} , is such that its action on the density vector r is the same as the action of the combination of the operators H , a_1 , a_1^\dagger , a_2 , a_2^\dagger on the density matrix ρ in equation (13). Since r is $(K_{max}+1)^4$ by 1, \mathcal{A} will be $(K_{max}+1)^4$ by $(K_{max}+1)^4$. The ordering of the operators is crucial.

For simplicity we explain it for the one mode case and the two mode case which is of interest to us in this paper is straightforward generalisation. In general, if the operator B acts on the left of a one mode ρ , the corresponding appropriate matrix \mathcal{B} is obtained by putting $K_{max}+1$ copies of B along the leading diagonal:

$$\mathcal{B}_{kl} = \begin{cases} B_{mn} & \text{if } k = p(K_{max}+1) + m, \\ & l = p(K_{max}+1) + n, \\ & \text{where } 0 \leq p, m, n \leq K_{max} \\ 0 & \text{otherwise.} \end{cases} \quad (27)$$

For example, the matrix equation

$$B\rho = \begin{pmatrix} a & c \\ b & d \end{pmatrix} \begin{pmatrix} w & y \\ x & z \end{pmatrix} = \begin{pmatrix} aw + cx & ay + cz \\ bw + dx & by + dz \end{pmatrix} \quad (28)$$

becomes the vector equation

$$\mathcal{B}r = \begin{pmatrix} a & c \\ b & d \\ & a & c \\ & & b & d \end{pmatrix} \begin{pmatrix} w \\ x \\ y \\ z \end{pmatrix} = \begin{pmatrix} aw + cx \\ bw + dx \\ ay + cz \\ by + dz \end{pmatrix}. \quad (29)$$

If the operator C acts on the right of the one mode ρ , the corresponding appropriate matrix \mathcal{C} is given by interlacing inflated copies of the *transpose* of C (not C^\dagger) along the leading diagonal:

$$\mathcal{C}_{kl} = \begin{cases} C_{nm} & \text{if } k = p + m(K_{max}+1), \\ & l = p + n(K_{max}+1), \\ & \text{where } 0 \leq p, m, n \leq K_{max} \\ 0 & \text{otherwise.} \end{cases} \quad (30)$$

For example, the matrix equation

$$\rho C = \begin{pmatrix} w & y \\ x & z \end{pmatrix} \begin{pmatrix} a & c \\ b & d \end{pmatrix} = \begin{pmatrix} aw + by & cw + dy \\ ax + bz & cx + dz \end{pmatrix} \quad (31)$$

becomes

$$\mathcal{C}r = \begin{pmatrix} a & b \\ a & b \\ c & d \\ c & d \end{pmatrix} \begin{pmatrix} w \\ x \\ y \\ z \end{pmatrix} = \begin{pmatrix} aw + by \\ ax + bz \\ cw + dy \\ cx + dz \end{pmatrix}. \quad (32)$$

References

1. G. Schon, A.D. Zaikin Phys. Rep. **198**, 237 (1990); M.A. Kastner, Rev. Mod. Phys. **64**, 849 (1992); T.P. Spiller, T.D. Clark, R.J. Prance, A. Widom, Prog. Low Temp. Phys. **13**, 219 (1992); *Single-charge tunneling*, NATO ASI series, Vol. 294, edited by H. Grabert, M.H. Devoret (Plenum, NY, 1992); Y. Makhlin, G. Schon, A. Shnirman, Rev. Mod. Phys. **73**, 357 (2001); R. Fazio, H. vanderZant, Phys. Rep. **355**, 235 (2001)
2. H.S.J. van der Zant, F.C. Fritschy, T.P. Orlando, J.E. Mooij Europhys. Lett. **18**, 343 (1992); A. van Oudenaarden, J.E. Mooij, Phys. Rev. Lett. **76**, 4947 (1996); A. van Oudenaarden, S.J.K. Vardy, J.E. Mooij, Phys. Rev. Lett. **77**, 4257 (1996); J.S. Chung, K.H. Lee, D. Stroud, Phys. Rev. B **40**, 6570 (1989); M. Octavio, J.U. Free, S.P. Benz, R.S. Newrock, D.B. Mast, C.J. Lobb, Phys. Rev. B **44**, 4601 (1991); L.L. Sohn, M.S. Rzchowski, J.U. Free, M. Tinkham, C.J. Lobb, Phys. Rev. B **45**, 3003 (1992)
3. A. Larkin, Y.N. Ovchinnikov, A. Schmid, Physica B **152**, 266 (1988); U. Eckern, A. Schmid, Phys. Rev. B **39**, 6441 (1989); J.S. Chung, K.H. Lee, D. Stroud, Phys. Rev. B **40**, 6570 (1989); F. Faló, A.R. Bishop, P.S. Lomdahl, Phys.

- Rev. B **41**, 10983 (1990); R. Fazio, G. Schon Phys. Rev. B **43**, 5307 (1991); S.P. Benz, C.J. Burroughs, Appl. Phys. Lett. **58**, 2162 (1991); A.V. Ustinov, T. Doderer, B. Mayer, R.P. Huebener, A.A. Galubov, V.A. Oboznov, Phys. Rev. B **47**, 944 (1993); S.G. Lachenmann, T. Doderer, D. Hoffmann, R.P. Huebener, P.A.A. Booij, S.P. Benz, Phys. Rev. B **50**, 3158 (1994)
4. L.L. Sohn, M.T. Tuominen, M.S. Rzchowski, J.U. Free, M. Tinkham, Phys. Rev. B **47**, 975 (1993); M. Franz, S. Teitel, Phys. Rev. B **51**, 6551 (1995); V.P. Koshelets, S.V. Shitov, A.V. Shchukin, L.V. Filippenko, J. Mygind, A.V. Ustinov, Phys. Rev. B **56**, 5572 (1997); A.V. Ustinov, B.A. Malomed, S. Sakai, Phys. Rev. B **57**, 1196 (1998); P. Barbara, A.B. Cawthorne, S.V. Shitov, C.J. Lobb Phys. Rev. Lett. **82**, 1963 (1999); A.B. Cawthorne, P. Barbara, S.V. Shitov, C.J. Lobb, K. Wiesenfeld, A. Zangwill, Phys. Rev. B **60**, 7575 (1999)
 5. B.J. van Wees, Phys. Rev. Lett. **65**, 255 (1990); Phys. Rev. B **44**, 2264 (1991); T.P. Orlando, K.A. Delin, Phys. Rev. B **43**, 8717 (1991); W.J. Elion, J.J. Wachtters, L.L. Sohn, J.E. Mooij, Phys. Rev. Lett. **71**, 2311 (1993)
 6. A. Widom, G. Megaloudis, T.D. Clark, R.J. Prance, H. Prance, J. Phys. A **15**, 3877 (1982); T.P. Spiller, T.D. Clark, R.J. Prance, H. Prance, D.A. Poulton, Nuovo Cim. B **105**, 43 (1990); R.J. Prance, H. Prance, T.P. Spiller, T.D. Clark, Phys. Lett. A **166**, 419 (1992)
 7. S.M. Girvin, Science **274**, 524 (1996); S.L. Sondhi, S.M. Girvin, J.P. Canini, D. Shahar, Rev. Mod. Phys. **69**, 315 (1997); M.P.A. Fisher, P.B. Weichman, G. Grinstein, D.S. Fisher, Phys. Rev. B **40**, 546 (1989); L.J. Geerligs, M. Peters, L.E.M. de Groot, A. Verbruggen, J.E. Mooij, Phys. Rev. Lett. **63**, 326 (1989); H.S.J. van der Zant, W.J. Elion, L.J. Geerligs, J.E. Mooij, Phys. Rev. B **54**, 10081 (1996)
 8. H.A. Krammers, G. Wannier, Phys. Rev. **60**, 252 (1941); L. Onsager, Phys. Rev. **65**, 117 (1944); G. Wannier, Rev. Mod. Phys. **17**, 50 (1945)
 9. G. t'Hooft, Nucl. Phys. B **153**, 141 (1979); in *Proc. 1980 Scottish Universities Summer School*, edited by K.C. Bowler, D.G. Sutherland (Redwood Burn, Edinburgh, 1981)
 10. J. Preskill, L.M. Kraus, Nucl. Phys. B **341**, 50 (1990); S. Coleman, J. Preskill, F. Wilczek, Phys. Rev. Lett. **67**, 1975
 11. A. Vourdas, Europhys. Lett. **48**, 201 (1999); A. Vourdas, T.P. Spiller, T.D. Clark, D. Poulton, Phys. Rev. B **63**, 104501 (2001)
 12. A. Vourdas, Phys. Rev. B **49**, 12040 (1994); L.M. Kuang, Y. Wang, M.L. Ge, Phys. Rev. B **53**, 11764 (1996); A.A. Odintsov, A. Vourdas, Europhys. Lett. **34**, 385 (1996); S. Bin, Z. Jian, X.S. Xing Xiu, Z. Phys. B **104**, 439 (1997); Z. Jian, S. Bin, X.S. Xing, Phys. Rev. B **56**, 14116 (1997); J.A. Vourdas, T.P. Spiller, Z. Phys. B **102**, 43 (1997); Z. Jian, S. Bin, Phys. Rev. B **64**, 024511 (2001); R. Migliore, A. Messina, A. Napoli, Int. J. Mod. Opt. B **14**, 3104 (2000); R. Migliore, A. Messina, A. Napoli, J. Opt. B **3**, 29 (2001); W.A. Al-Saidi, D. Stroud, Phys. Rev. B **65**, 014512 (2001)
 13. A. Konstadopoulou, J.M. Hollingworth, M. Everitt, A. Vourdas, T.D. Clark, J.F. Ralph, IEE Proc. Science, Meas. Tech. **148**, 229 (2001)
 14. T.P. Orlando, J.E. Mooij, L. Tian, C.H. van der Wal, L.S. Levitov, S. Lloyd, J.J. Mazo Phys. Rev. B **60**, 15398 (1999); Y. Makhlin, G. Schon, A. Shnirman, Nature (London) **398**, 305 (1999)
 15. Y. Nakamura, Y.A. Pashkin, J.S. Tsai Nature **398**, 786 (1999); J.R. Friedman *et al.*, Nature **406**, 43 (2000); van der Wal *et al.*, Science **290**, 773 (2000)
 16. A.J. Leggett *et al.*, Rev. Mod. Phys. **59**, 1 (1987); U. Weiss *Quantum Dissipative Systems* (World Scientific, Singapore, 1999); M.P.A. Fisher, W. Zwerger, Phys. Rev. B **32**, 6190 (1985)
 17. G. Lindbland, Commun. Math. Phys. **33**, 305 (1973); E.H. Lieb, Bull. Am. Math. Soc. **81**, 1 (1975); A. Wehrl, Rev. Mod. Phys. **50**, 221 (1978); S.M. Barnett, S.J.D. Phoenix, Phys. Rev. A **44**, 535 (1991); A. Vourdas, Phys. Rev. A **46**, 442 (1992)
 18. N.J. Cerf, C. Adami, Phys. Rev. Lett. **77**, 5194 (1997); N.J. Cerf, C. Adami, Physica D **120**, 62 (1998)
 19. E.T. Jaynes, F.W. Cummings, Proc. IEEE **51**, 89 (1963)
 20. P. Lancaster, M. Tismenetsky, *The theory of matrices* (London, Academic Press, 1985)